IEEE Access
Multidisciplinary | Rapid Review | Open Access Journal

Received December 13, 2019, accepted January 14, 2020, date of publication January 20, 2020, date of current version January 30, 2020.

Digital Object Identifier 10.1109/ACCESS.2020.2968218

Design and Testing of Cantilevered PVDF Energy Harvester Based on the Coanda Effect

XIAOHUI LU[1,2], QIANG GAO[2], YINGTING WANG[3], XIANPENG FU[2,4], PING WANG[1,5], TINGHAI CHENG[2], AND CHUANXUE SONG[1]

[1]State Key Laboratory of Automotive Simulation and Control, Jilin University, Changchun 130025, China
[2]School of Mechatronic Engineering, Changchun University of Technology, Changchun 130012, China
[3]School of Mechatronic Engineering, Harbin Institute of Technology, Harbin 150000, China
[4]Beijing Institute of Nanoenergy and Nanosystems, Chinese Academy of Sciences, Beijing 100083, China
[5]Department of Control Science and Engineering, Jilin University, Changchun 130025, China

Corresponding authors: Xiaohui Lu (luxh13@ccut.edu.cn) and Ping Wang (wangping12@jlu.edu.cn)

This work was supported in part by the State Key Laboratory of Automotive Simulation and Control (Jilin University) under Grant 20171116, and in part by the National Nature Science Foundation of China under Grant 51775130 and Grant 61603060.

ABSTRACT Low-flow air has been attracted many researchers which can be transformed into electric energy by the piezoelectric materials. A flow amplifier device can be used to increase the performance of piezoelectric energy harvester excited by low-flow air. The Coanda effect theory has been analyzed based on the fast-moving air. To analyze the effect of the amplifier device and verify the feasibility of the proposed cantilevered PVDF energy harvester, we employed finite element simulation to analyze the flow distribution of the amplified flow air. Then the stress and potential distribution of PVDF film have been analyzed. A prototype of the cantilevered PVDF energy harvester is tested with different variables such as input air flow, pressure and cycle time. The test results show that the output voltage increases with increasing input air flow. The output voltage decreases slightly with increasing input cycle time. The peak voltage decreases as the distance between the prototype and the excitation source increases. Importantly, the output voltage for the amplified airflow is about three-times that of the non-amplified air flow. The maximal output voltage and power are 12.80 V and 19.89 μW at the pressure of 0.2 MPa and a flow rate of 200 L/min, respectively.

INDEX TERMS Coanda effect, PVDF energy harvester, amplified air flow, simple harmonic oscillation.

I. INTRODUCTION

Harvesting energy from the ambient environment has always been a hot issue and a possible solution against the energy crisis [1], [2]. Recently, a kind of new energy harvesting device has attracted more and more attention owing to its simple design, low cost, reliable robustness, environmentally friendliness and abundant friction energy sources [3], [4]. A series of great progress have been developed on micro-power generators with thermoelectric, thermo-photovoltaic, piezoelectric, and microbial fuel cells [5]–[10]. Some of this research has been devoted to improving energy harvesting efficiency, to provide stable energy for self-powered wireless electronic devices [11]–[13]. This would eliminate the issue of battery replacement and disposal [14]–[16]. The air kinetic energy is an abundant and freely available energy source. Previous researchers have designed effective systems to convert ambient air kinetic energy into electricity for wireless sensors [17]–[20].

The flexibility associated with piezoelectric materials is very attractive for energy harvesting. These materials possess more mechanical energy for conversion into electrical energy and can also withstand large amounts of strain [21]–[23]. Polyvinylidene fluoride (PVDF) is a highly flexible piezoelectric material that can improve the service life of the piezoelectric generator [24]. Many studies have explored the performance of PVDF under different air impact conditions. Mo et al. presented a comprehensive theoretical model for predicting the energy generation performance of an energy harvesting device that used a PVDF circular membrane subject to pressure fluctuations [25]. Yu et al. presented the flapping dynamics of a PVDF membrane placed behind a cylinder. Their harvester was extensively studied in subcritical and postcritical regimes by changing the distance between the cylinder and the membrane [26]. Chen *et al.* proposed a beating design using PVDF in collaboration with a beating mechanism [27]. Tang *et al.* proposed a novel wind energy

The associate editor coordinating the review of this manuscript and approving it for publication was Jingfeng Song.

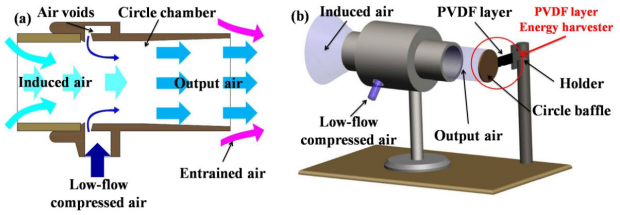

FIGURE 1. Diagrams showing (a) the working principle of flow amplifier device, and (b) the amplified air flow impact.

harvester using a wind vane and PVDF film to convert the multidirectional wind energy in the grid into electricity [28]. Eddiai *et al.* has been researched to provide a framework to develop an innovative energy-harvesting technology that collects vibrations from the environment and converts them into electricity to power a variety of sensors [29]. The low-flow compressed air condition has always existed in pneumatic systems, but this energy is often overlooked and wasted. Based on the low-flow compressed air energy, an amplifier device can be designed to harvest air energy composed of kinetic energy and compressed energy.

The energy collection device of airfoil structure has been studied in previous papers which is based on Coanda effect [28]. In this paper, the Coanda effect theory has been analyzed based on the fast-moving air. To analyze the effect of the amplifier device and verify the feasibility of the proposed cantilevered PVDF energy harvester, we employed finite element simulation to analyze the flow distribution of the amplified flow air. Then the stress and potential distribution of PVDF film have been analyzed. A flow amplifier device is fabricated to amplify low-flow compressed air through the Coanda effect. A cantilevered PVDF energy harvester is designed to extract energy from an amplified flow. The aim of this paper is to enhance the generation performance of a cantilevered PVDF energy harvester which is impacted by amplified air flow. The energy harvester consists of a flexible PVDF, a polyester substrate and a circular baffle without any other structural components. The test system is built and the experiments are designed to explore the relationships between the generated power and the low-flow compressed air parameters. In short, this primary study shows a promising scheme for guiding the future development of high-efficiency piezoelectric harvesters.

II. STRUCTURE AND SIMULATION ANALYSIS

Figure 1 shows the working principle of the flow amplifier device and the diagrammatic drawing of the amplified air flow impact. Figure 1(a) shows the working principle of the flow amplifier device. The low-flow compressed air is provided by a pneumatic system and the compressed air can through the air voids. As the air voids is small enough, the compressed air spills into the cylindrical chamber at high speed. The pressure in the cylindrical chamber decreases owing to the high-speed air. The ambient air is induced by the pressure difference; this region of the air flow is hereafter

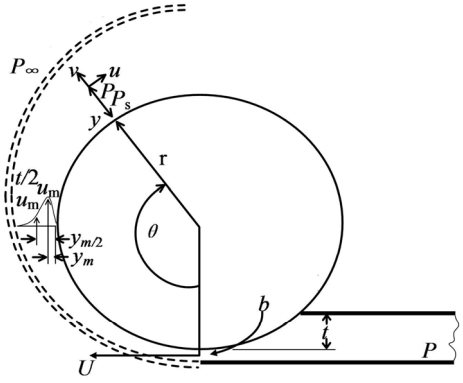

FIGURE 2. Schematic diagram of turbulent flow around cylindrical surface.

called induced air. The induced air obviously increases the flow of the output air, and the output air is thus amplified. Additionally, some entrained air is induced by the output air at the exit, but this has only a small influence. Figure 1(b) shows the amplified airflow impact. When the air impacts the circle baffle, electricity is produced by the deformation of the PVDF. A circular baffle has been designed in the harvester to increase the air impact area.

The basic principle of the Coanda effect is that the friction resistance on the convex surface will cause pressure difference on both sides of the fluid, making the pressure attached to the wall surface less than that on the other side. Under the action of the pressure difference, the fluid will deflect to the side in low pressure to achieve a stable flow state adhered to the wall. There are two necessary conditions for the fluid with low viscosity such as air to reflect the Coanda effect. First, the wall surface is required to allow the fluid to adhere, and it needs to have a certain curvature or be at a certain angle to the direction of the jet flow in the pipe. Secondly, the jet nozzle and both sides of the wall surface should have a certain distance so as to generate a certain pressure difference Δp on both sides of the fluid. Researchers studied a turbulent jet flow that flows around the cylindrical surface by adhering to it. The fluid was an ideal incompressible fluid. The schematic diagram of its principle is shown in Figure 2.

In nature, the fluid will flow with the curvature of the wall because of the viscous force. The Coanda effect is based on the wall attached due to the air viscosity. When the fluid comes into contact with the surface of the cylinder, the viscous resistance on the outer surface will make the fluid to decelerate. The pressure of the fluid on the surface of the cylinder is p_s, while p_s is less than the pressure of the surrounding fluid p_∞, which will cause the fluid to flow around the cylindrical surface by adhering to it. Assuming that the fluid is inviscid in its initial state, we will obtain the equation by using the Bernoulli equation for fluid flow:

$$p_s = p_\infty - \frac{2\rho U b}{a} \tag{1}$$

In the equation, ρ is the density of the jet fluid, U is the average speed of the fluid, b is the width of the orifice, a is the radius of the curved wall. In an inviscid fluid, the value $2\rho Ub/a$ is much lower than p_∞. However, the actual fluid has viscosity. The viscosity of the fluid will lead to the decrease of the flow velocity. The fluid acting on the wall surface will produce the pressure. This part of pressure gradually decrease with the decrease of the flow velocity. When p_s equals to p_∞, The fluid will break away from the wall surface it used to adhere to. The pressure distribution when the fluid flows on the wall surface can be expressed as:

$$\frac{(p_s - p_{surf})\, r}{(p - p_s)\, b} = \frac{8 \ln\left(1 + \frac{4y_{m/2}}{3r}\right)}{\left[\left(1 + \frac{4y_{m/2}}{3r}\right)^2 - 1 + 2\ln\left(1 + \frac{4y_{m/2}}{3r}\right)\right]} \tag{2}$$

The separation angle can be expressed as:

$$\theta_{sep} = \frac{(245 - 391b/r)}{(1 + 1.125b/r)} \tag{3}$$

Parameter relations in the Newman model:

$$\frac{y_{m/2}}{r\theta} = 0.11\left(1 + 1.5\frac{y_{m/2}}{r}\right) \tag{4}$$

In the equation, θ is the separation angle, b is the width of the jet opening, a is the radius of curvature. The main factor of the Coanda effect is the change of velocity of which flows in the contact surface. There are many factors affect the velocity of contact surface fluid. This paper mainly discusses the influence of flow state and pressure distribution on Coanda effect. We could know from the mathematical expression R_e equal to $\rho vd/\eta$ of Reynolds number and the effect of flow state on Coanda effect is essentially the effect of Reynolds number on the layer adhered to the wall. When the fluid is in the turbulent flow state, the thickness of the layer adhered to the wall can be increased, and the thicker layer will make the turbulent fluid more difficult to detach from the wall surface than laminar fluid. In the process of fluid flow, the pressure gradient affects the critical Reynolds number, and the change of the pressure gradient in the flow direction will significantly affect the flow state of the attached wall layer. The positive pressure gradient is favorable for the fluid to adhere to the wall and is not easy to produce the shedding phenomenon. The adverse pressure gradient is easy to cause fluid shedding. Brandt laminar wall equation reflects the effect of pressure gradient on fluid adhesion.

$$\frac{\partial u_x}{\partial x} + \frac{\partial u_y}{\partial y} = 0 \tag{5}$$

$$\frac{\partial u_x}{\partial t} + u_x\frac{\partial u_x}{\partial x} + u_y\frac{\partial u_y}{\partial y} = -\frac{1}{\rho}\frac{\partial p}{\partial x} + \frac{u}{\rho}\frac{\partial^2 u_x}{\partial y^2} \tag{6}$$

The above equation satisfies the following conditions

$$y = 0, \quad u_x = u_y = 0 \tag{7}$$

$$y = \infty, \quad u = u(x) \tag{8}$$

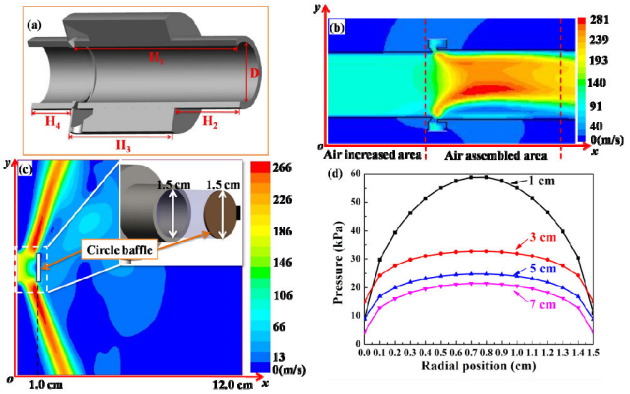

FIGURE 3. Model dimensions and flow distribution. (a) Primary dimensions of the amplifier device, (b) flow distribution of the induced amplified flow air, (c) flow distribution of the external air flow, and (d) pressure distribution at the circular baffle surface at different distances.

The equation (9) can be described based on the equation (7),

$$\mu\left(\frac{\partial u}{\partial y}\right)_{y=0} = \frac{dp}{dx} \tag{9}$$

In the reverse pressure gradient region,

$$\frac{dp}{dx} > 0, \quad \left(\frac{\partial^2 u}{\partial y^2}\right)_{y=0} > 0 \tag{10}$$

To analyze the effect of the amplifier device and verify the feasibility of the proposed cantilevered PVDF energy harvester, we employed finite element simulation to analyze the flow distribution of the amplified flow air, as shown in the model in Figure 3. The lengths of H_1, H_2, H_3 and H_4 are 5.7 cm, 1.5 cm, 4.5 cm and 1.5 cm, respectively. The diameter D of the cylindrical chamber is 1.5 cm. In Figure 3(b), there are two areas named ''air increased area'' and ''air assembled area''. The simulation results show that the output air is amplified by the amplifier device. Figure 3(c) shows the flow distribution of the external air flow when the circular baffle is placed at 1 cm from air exit. The maximum flow speed is 266 m/s when the distance is 1 cm. Figure 3(d) shows the pressure distribution on the circular baffle surface at different distances. The center of the circular baffle has the highest pressure, and the edge of the circular baffle has the smallest pressure. The pressure shows a downward trend from the center to the edge of the circular baffle. The distance of 1 cm has the largest impact force of nearly 60 kPa. According to the simulation result, the baffle should be fixed at 1.0 cm.

After completing the simulation analysis of the external and internal flow field distribution in the air amplifier, the pressure field distribution on the surface of the circular spoiler was obtained. Based on that, the stress and potential distributions of PVDF thin film piezoelectric captors are calculated. When the PVDF thin film piezoelectric energy capture device is fixed 1 cm away from the end of the air amplifier, the pressure load acting on the circular spoiler

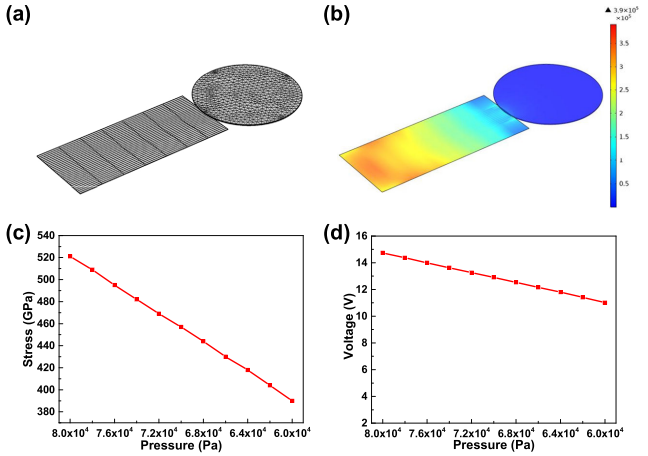

FIGURE 4. The electro-mechanical analysis of the piezoelectric energy capture device. (a) The mesh generation of the device, (b) stress distribution of the device and the impact of pressure on the (c) stress and (d) voltage.

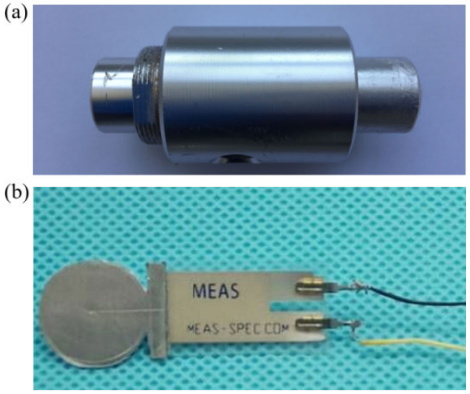

FIGURE 5. Real photo of circular spoiler piezoelectric energy capture device.

is 60 kPa. Figure 4 shows the stress and potential distribution of PVDF film piezoelectric energy captor under this pressure load. According to the flow field environment, the electrical simulation analysis is carried out. Then we used the Comsol analyze the electro-mechanical of it with the analysis result of Fluent. Figure 4(a) shows the mesh generation of the device and the stress distribution is shown in Figure 4(b) when a 6.0×10^4 Pa pressure act on the device. The impact of pressure on the stress and voltage are illustrated in Figure 4(c) and (d), respectively, they are decreasing with the pressure decrease.

Simulation results show that the design of air amplifier is reasonable, and the air amplifier as shown in Figure 5 (a) was selected. The jet orifice diameter of the air amplifier is 15 mm, so that the jet fluid of the air amplifier can be more fully impacted on the circular spoiler. According to the size of the air amplifier jet port, the size of the selected PVDF film is $23.5 \times 10 \times 0.028$ mm^3, and its dynamic resistance can be measured through the analysis of the impedance tester. A round spoiler with a diameter of 15 mm is bonded to the top of the PVDF film to increase the wind area of

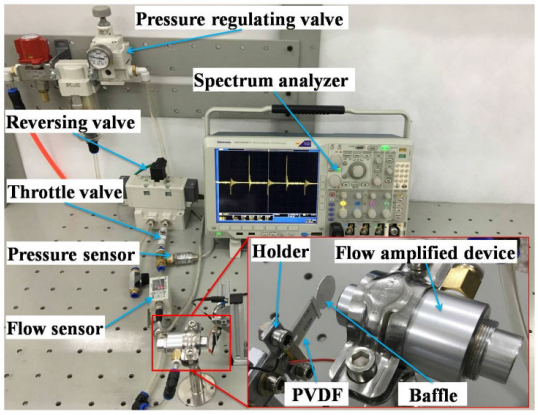

FIGURE 6. Experimental setup of the cantilevered PVDF energy harvester.

the piezoelectric energy capture. The structure is shown in Figure 5(b). The width of the overlap between the PVDF film and the spoiler was 2 mm, and the thickness of the colloid was 0.8 mm. The diameter of the air amplifier jet port is 15 mm, and the diameter of the internal channel is 13 mm, which can increase the flow rate of the air supply flow by more than 4 times.

III. EXPERIMENTAL SYSTEM

The experimental setup of the cantilevered PVDF energy harvester is shown in Figure 6. The test system consists of a pressure regulating valve (IR3020-04 SMC Japan), a reversing valve (VQ7-8-FG SMC Japan), a throttle valve (AS2052F SMC Japan), a flow sensor (PFA751-04 SMC Japan), a pressure sensor (PSE560-01 SMC Japan), and the prototype. The output voltage is monitored via a four-channel spectrum analyzer (MDO4054B-3 Tektronix USA) using a probe (TPP0500 Tektronix USA). The low-flow compressed air is transferred from the pressure regulating valve to the reversing valve through the tube. When the air flows into the throttle valve, the air flow can be adjusted. In this system, the volume flow is tested using the flow sensor and the pressure is tested via the pressure sensor. An enlarged view of the cantilevered PVDF energy harvester and flow amplifier device is inset in Figure 6. The cantilevered PVDF energy harvester consists of a flexible PVDF (Measurement Specialties, Hampton, VA, USA), a polyester substrate and a circular baffle.

The energy harvester is impacted by a stable air flow. In the test, the pressure and flow are adjusted by regulating the pressure and throttle, respectively. There are two other parameters in the test system, namely distance and cycle. Experiments are carried out to investigate the characteristic of the proposed prototype under various parameters in the test system.

IV. RESULTS AND DISCUSSION

Figure 7 shows the peak voltage of the harvester in different cycles and pressures. Figure 7(a) shows the test results for the peak voltage of the harvester at 200 L/min and

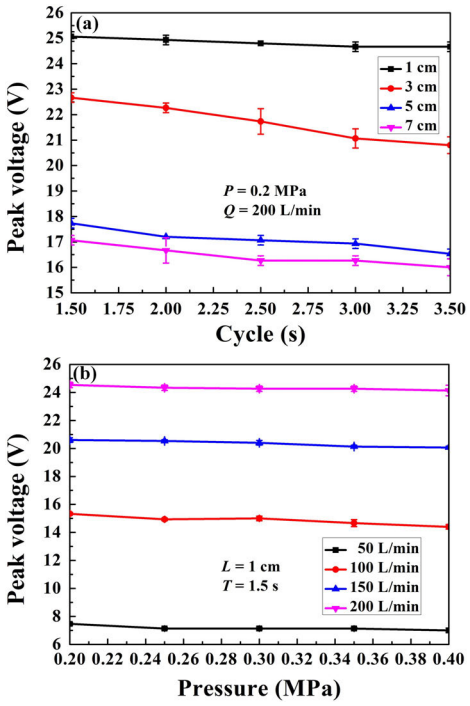

FIGURE 7. Peak voltages from the harvester in (a) different cycles, and (b) different pressures in different flows.

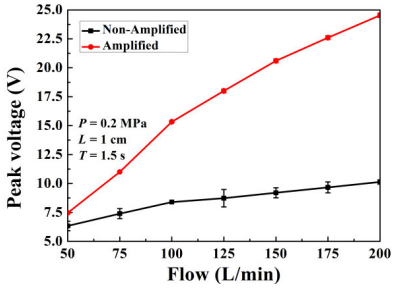

FIGURE 8. The relationship between the flow and the peak voltage.

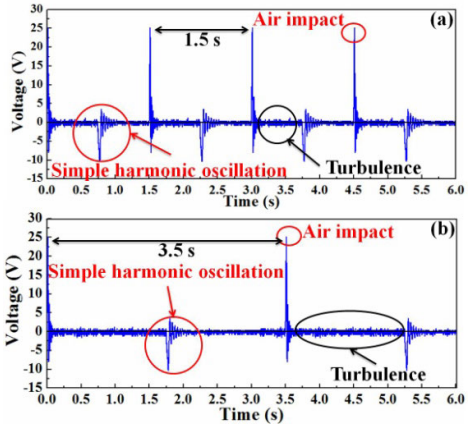

FIGURE 9. Change in voltage for a cycle time of (a) 1.5 sand (b) 3.5 s.

0.2 MPa. Different distance between the baffle and flow amplified device has been selected by 1, 3, 5, 7 cm. The maximum peak voltage is 25.07 V at 1.0 cm and 0.2 MPa for a cycle time of 1.5 s. All of the data points are measured more than twenty times and the mean voltages are plotted along with appropriate error bars, within the error allowed.

Figure 7(a) indicates that the peak voltage decreases with increasing cycles. In that case, the peak voltage must be influenced by the gas velocity. However, while the cycles are increased, the velocity in the air pipe decreases when the flow is fixed. As a result, the peak voltage is also reduced. The relationships between the various air pressures and peak voltages are investigated as shown in Fig.7 (b). The experimental parameters are 0.2 MPa, 1 cm, and cycle of 1.5 s. To investigate the effect of the air flow on the performance of the harvester, different flows of 50 L/min, 100 L/min, 150 L/min and 200 L/min are used to amplify the different increased air flows. The peak voltage increases with increasing flow. As the input pressure increases, the peak voltage decreases and the curves indicate that the peak voltages also decrease slowly. A maximum peak voltage of 24.53 V was achieved at 200 L/min for the smallest cycle time.

The air amplifier can absorb air at the back end to increase the flow rate. The output voltage is small when blocking the end of air for test. Figure 8 shows the relationship between the flow and the peak voltage under the cycle of 1.5 s, 1 cm, and 0.2 MPa. The peak voltage for the amplified air flow is shown in the amplified flow curve. The peak voltage for the low-flow compressed air is shown in the non-amplified flow curve. The pressure has previously been defined as 0.2 MPa with a higher peak voltage. The cycle time is set at 1.5 s and the distance is set at 1.0 cm. The peak voltage increases when the flow increases. The maximum peak voltage is 24.53 V at 200 L/min.

Figure 8 indicates that the peak voltage for amplified air is approximately three-times that of the non-amplified air. It indicates that amplified flow can improve the power output effectively.

For test conditions fixed at 0.2 MPa, 200 L/min and 1 cm, Figure 9 shows the change in voltage with time for a cycle time of (a) 1.5 s and (b) 3.5 s. The whole process of power generation can be divided into three stages: forced oscillation, turbulence, and simple harmonic oscillation. The PVDF deforms when the air flow impacts on the circular baffle. The PVDF undergoes forced oscillation until it becomes stable in the equilibrium position. When the PVDF is in the equilibrium position, it enters the turbulence stage. After the turbulence stage, the PVDF enters simple harmonic oscillation.

In Figure 9, the air pressure is continuously supplied for 1.5 and 3.5 seconds. The time of simple harmonic oscillation is 0.30 s which is no air impact. The time of simple harmonic oscillation depends on the characteristics of the PVDF energy harvester. The amplitude of the turbulent section is very small. As a result, the output voltages are almost zero. Thus, we can speculate that the power output is getting smaller as the cycle time is increased.

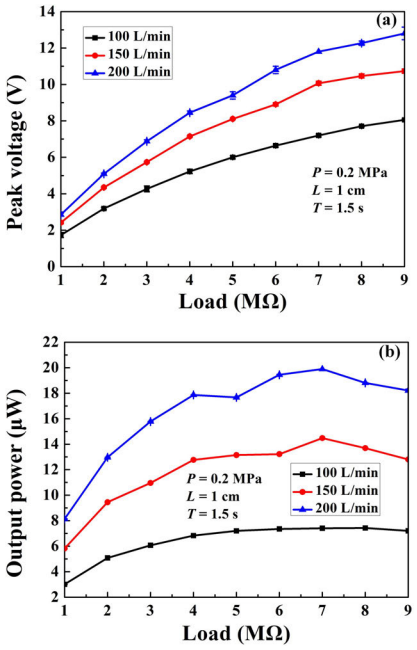

FIGURE 10. Graphs showing (a) peak voltage and (b) power output versus load resistance for cycle times of 1.5 s.

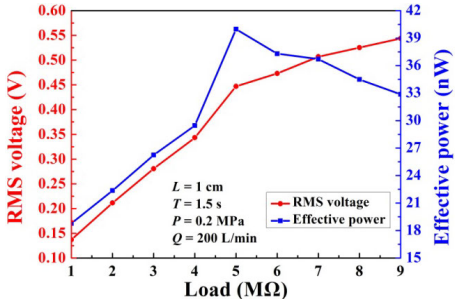

FIGURE 11. Root means square (RMS) voltage and effective power versus load resistance using cycle times of 1.5 s, a process pressure of 0.2 MPa and a flow rate of 200 L/min.

Figure 10(a) shows the peak voltage versus load resistance for a cycle time of 1.5 s. The peak voltage increases with increasing external resistance for a given flow rate, while the peak voltage output across the load increases with increasing of the flow rate. The maximum peak voltage achieved is 12.80 V across 9 MΩ resistors at 0.2 MPa and 200 L/min for the smallest cycle time (1.5 s). Figure 10(b) shows the power output versus load resistance for a cycle time of 1.5 s. The optimal instantaneous power output is 19.89 μW through a 7 MΩ resistor at 0.2 MPa and 200 L/min for a cycle time of 1.5 s.

The root means square (RMS) voltage is excited for a cycle time of 1.5 s, as shown in Figure 11. The conditions of these curves are tested using the above excitation distance of 1 cm, a process pressure of 0.2 MPa and a flow rate of 200 L/min. The RMS voltage and the effective power against the external load resistance are measured, and it is found that the RMS voltage increases with the increasing of load resistance. The maximal RMS voltage is 0.54 V across a resistance of 9 MΩ. The optimal effective power is 39.97 nW through a resistance of 5 MΩ. At the same time, according to the size of the selected PVDF film, the energy density of the energy harvester can be obtained to be 6.0 μW/cm^3.

V. CONCLUSION

In conclusion, this paper presented a method by which the power output of a PVDF energy harvester is improved by amplified air flow. The Coanda effect is used to amplify the air flow. The Coanda effect theory has been analyzed based on the fast-moving air. To analyze the effect of the amplifier device and verify the feasibility of the proposed cantilevered PVDF energy harvester, we employed finite element simulation to analyze the flow distribution of the amplified flow air. Then the stress and potential distribution of PVDF film have been analyzed. The flow distributions depending on the positions of baffle when the amplified flow impacts on it. A PVDF energy harvester which is impacted by amplified air flow is fabricated and tested. The maximum peak voltage reaches 12.80 V across a 9 MΩ resistor at 200 L/min and 0.2 MPa for a cycle time of 1.5 s. The optimal instantaneous power output is 19.89 μW through a 7 MΩ resistor at 0.2 MPa and 200 L/min for a cycle time of 1.5 s. The relationship between flow speed and voltage is an important index. This will be tested in detail in future work.

Importantly, the output voltage for the amplified air flow increased to about three-times that for non-amplified flow. Thus, the low-flow compressed air in the pneumatic system has great potential despite the power output is slightly lower. In short, this primary study shows a promising scheme for guiding the future design. This paper mainly analyzes the influence of Coanda effect on piezoelectric patch. Thus, the original structure is selected to research the performance of power generation. We will optimize the structure design in the following work.

REFERENCES

[1] H. Mutsuda, Y. Tanaka, R. Patel, and Y. Doi, "Harvesting flow-induced vibration using a highly flexible piezoelectric energy device," *Appl. Ocean Res.*, vol. 68, pp. 39–52, Oct. 2017.

[2] W. Yang and S. Towfighian, "A parametric resonator with low threshold excitation for vibration energy harvesting," *J. Sound Vib.*, vol. 446, pp. 129–143, Apr. 2019.

[3] C. Bruni, J. Gibert, G. Frulla, E. Cestino, and P. Marzocca, "Energy harvesting from aeroelastic vibrations induced by discrete gust loads," *J. Intell. Mater. Syst. Struct.*, vol. 28, no. 1, pp. 47–62, Jan. 2017.

[4] G. Zhang, S. Gao, H. Liu, and W. Zhang, "Design and performance of hybrid piezoelectric-electromagnetic energy harvester with trapezoidal beam and magnet sleeve," *J. Appl. Phys.*, vol. 125, no. 8, Feb. 2019, Art. no. 084101.

[5] A. Abasian, A. Tabesh, N. Rezaei-Hosseinabadi, A. Z. Nezhad, M. Bongiorno, and S. A. Khajehoddin, "Vacuum-packaged piezoelectric energy harvester for powering smart grid monitoring devices," *IEEE Trans. Ind. Electron.*, vol. 66, no. 6, pp. 4447–4456, Jun. 2019.

[6] S. Chamanian, H. Ulusan, A. Koyuncuoglu, A. Muhtaroglu, and H. Kulah, "An adaptable interface circuit with multistage energy extraction for low-power piezoelectric energy harvesting MEMS," *IEEE Trans. Power Electron.*, vol. 34, no. 3, pp. 2739–2747, Mar. 2019.

[7] M. R. Sarker, R. Mohamed, M. H. M. Saad, and A. Mohamed, "DSPACE controller-based enhanced piezoelectric energy harvesting system using PI-lightning search algorithm," *IEEE Access*, vol. 7, pp. 3610–3626, 2019.

[8] A. Abdelkefi, J. M. Scanlon, E. Mcdowell, and M. R. Hajj, "Performance enhancement of piezoelectric energy harvesters from wake galloping," *Appl. Phys. Lett.*, vol. 103, no. 3, Jul. 2013, Art. no. 033903.
[9] N. Kaur and S. Bhalla, "Numerical investigations on energy harvesting potential of thin PZT patches adhesively bonded on RC structures," *Sens. Actuators A, Phys.*, vol. 241, pp. 44–59, Apr. 2016.
[10] T. Cheng, Y. Wang, F. Qin, Z. Song, X. Lu, G. Bao, and X. Zhao, "Piezoelectric energy harvesting in coupling-chamber excited by the vortex-induced pressure," *Appl. Phys. Lett.*, vol. 109, no. 7, Aug. 2016, Art. no. 073902.
[11] Y. Hu, X. Liang, and W. Wang, "A theoretical solution of resonant circular diaphragm-type piezoactuators with added mass loads," *Sens. Actuators A, Phys.*, vol. 258, pp. 74–87, May 2017.
[12] S. Saadon and O. Sidek, "A review of vibration-based MEMS piezoelectric energy harvesters," *Energy Convers. Manage.*, vol. 52, no. 1, pp. 500–504, 2011.
[13] A. Toprak and O. Tigli, "Piezoelectric energy harvesting: State-of-the-art and challenges," *Appl. Phys. Rev.*, vol. 1, Sep. 2014, Art. no. 031104.
[14] J. Chang, M. Dommer, C. Chang, and L. Lin, "Piezoelectric nanofibers for energy scavenging applications," *Nano Energy*, vol. 1, no. 3, pp. 356–371, May 2012.
[15] S. B. Lang, S. A. M. Tofail, A. L. Kholkin, M. Wojtas, M. Gregor, A. A. Gandhi, Y. Wang, S. Bauer, M. Krause, and A. Plecenik, "Ferroelectric polarization in nanocrystalline hydroxyapatite thin films on silicon," *Sci. Rep.*, vol. 3, p. 2215, Jul. 2013.
[16] S. Y. Xu, Y. W. Yeh, G. Poirier, M. C. McAlpine, R. A. Register, and N. Yao, "Flexible piezoelectric PMN–PT nanowire-based nanocomposite and device," *Nano Lett.*, vol. 13, no. 6, pp. 2393–2398, 2013.
[17] Z. Zhang, J. Kan, S. Wang, H. Wang, C. Yang, and S. Chen, "Performance dependence on initial free-end levitation of a magnetically levitated piezoelectric vibration energy harvester with a composite cantilever beam," *IEEE Access*, vol. 5, pp. 27563–27572, 2017.
[18] L. A. Weinstein, M. R. Cacan, P. M. So, and P. K. Wright, "Vortex shedding induced energy harvesting from piezoelectric materials in heating, ventilation and air conditioning flows," *Smart Mater. Struct.*, vol. 21, no. 4, Apr. 2012, Art. no. 045003.
[19] H. Dai, A. Abdelkefi, and L. Wang, "Theoretical modeling and nonlinear analysis of piezoelectric energy harvesting from vortex-induced vibrations," *J. Intell. Mater. Syst. Struct.*, vol. 25, no. 14, pp. 1861–1874, Sep. 2014.
[20] Y. Wang, L. Wang, T. Cheng, Z. Song, and F. Qin, "Sealed piezoelectric energy harvester driven by hyperbaric air load," *Appl. Phys. Lett.*, vol. 108, no. 3, Jan. 2016, Art. no. 033902.
[21] X. Chen, Y. Wang, K. Cai, Y. Bai, S. Bo, and D. Guo, "P(VDF-TrFE) nanorod assemblies with anisotropic piezoelectric properties investigated by piezoelectric response microscopy," *J. Appl. Phys.*, vol. 116, no. 6, Aug. 2014, Art. no. 066821.
[22] W.-S. Jung, M.-G. Kang, H. G. Moon, S.-H. Baek, S.-J. Yoon, Z.-L. Wang, S.-W. Kim, and C.-Y. Kang, "High output piezo/triboelectric hybrid generator," *Sci. Rep.*, vol. 5, p. 9309, Mar. 2015.
[23] V. V. Yashin, S. P. Levitan, and A. C. Balazs, "Achieving synchronization with active hybrid materials: Coupling self-oscillating gels and piezoelectric films," *Sci. Rep.*, vol. 5, p. 11577, Jun. 2015.
[24] N. Rezaei-Hosseinabadi, A. Tabesh, R. Dehghani, and A. Aghili, "An efficient piezoelectric windmill topology for energy harvesting from low-speed air flows," *IEEE Trans. Ind. Electron.*, vol. 62, no. 6, pp. 3576–3583, Jun. 2015.
[25] C. Mo, J. Davidson, and W. W. Clark, "Energy harvesting with piezoelectric circular membrane under pressure loading," *Smart Mater. Struct.*, vol. 23, no. 4, Apr. 2014, Art. no. 045005.
[26] Y. Yu and Y. Liu, "Flapping dynamics of a piezoelectric membrane behind a circular cylinder," *J. Fluids Struct.*, vol. 55, pp. 347–363, May 2015.
[27] H.-H. Huang and K.-S. Chen, "Design, analysis, and experimental studies of a novel PVDF-based piezoelectric energy harvester with beating mechanisms," *Sens. Actuators A, Phys.*, vol. 238, pp. 317–328, Feb. 2016.
[28] M. Tang, Q. Guan, X. Wu, X. Zeng, Z. Zhang, and Y. Yuan, "A high-efficiency multidirectional wind energy harvester based on impact effect for self-powered wireless sensors in the grid," *Smart Mater. Struct.*, vol. 28, no. 11, Nov. 2019, Art. no. 115022.
[29] A. Eddiai, M. Meddad, R. Farhan, M. Mazroui, M. Rguiti, and D. Guyomar, "Using PVDF piezoelectric polymers to maximize power harvested by mechanical structure," *Superlattices Microstruct.*, vol. 127, pp. 20–26, Mar. 2019.
[30] T. Cheng, X. Fu, W. Liu, X. Lu, X. Chen, Y. Wang, and G. Bao, "Airfoil-based cantilevered polyvinylidene fluoride layer generator for translating amplified air-flow energy," *Renew. Energy*, vol. 135, pp. 399–407, May 2019.

XIAOHUI LU was born in Jilin, China. She received the B.S. degree in mathematics and applied mathematics from Beihua University, Jilin, in 2004, the M.S. degree in operational research and cybernetics from the Lanzhou University of Technology, Lanzhou, China, in 2007, and the Ph.D. degree in control theory and application from Jilin University, Changchun, China, in 2013. She was a Visiting Scholar with the College of Engineering, The Ohio State University, under the supervision of Junmin Wang, from 2017 to 2018. She is currently an Associate Professor with the Changchun University of Technology and a Postdoctoral with Jilin University. Her current research interests include vehicle powertrain control, model predictive control, data-driven control, and triboelectric nanogenerators.

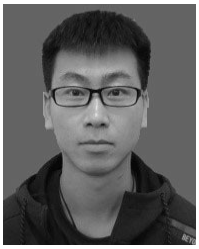

QIANG GAO was born in Shanxi, China, in 1994. He received the B.S. degree from the Luoyang Institute of Science and Technology, Luoyang, China, in 2018. He is currently pursuing the M.S. degree in mechanical engineering with the Changchun University of Technology. His research interests include friction drive mechanism and piezoelectric energy harvesting.

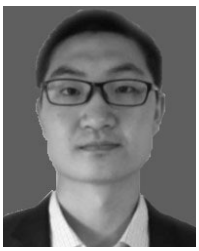

YINGTING WANG was born in Jilin City, China, in 1990. He received the B.E. degree in mechanical engineering from the Changchun University of Technology, in 2014. He is currently pursuing the Ph.D. degree with the Harbin Institute of Technology. His current main research interest includes the design and analysis of novel piezoelectric energy harvester and pneumatic technology.

XIANPENG FU was born in Anhui, China, in 1993. He received the B.S. and M.S. degrees in mechanical engineering and automation from the Changchun University of Technology, Changchun, China. He is currently with the Beijing Institute of Nanoenergy and Nanosystems, Chinese Academy of Sciences. His research interests include piezoelectric generators and triboelectric nanogenerators.

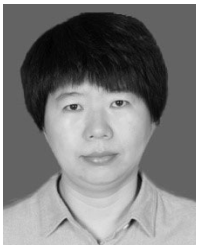

PING WANG received the M.Eng. and Ph.D. degrees from the Department of Control Science and Engineering, Jilin University, Changchun, China, in 2008 and 2011, respectively. From 2011 to 2015, she was an Assistant Professor with Jilin University, where she has been an Associate Professor, since November 2015. Her research interests include control theory and its applications in automotive powertrain.

TINGHAI CHENG received the B.S., M.S., and Ph.D. degrees from the Harbin Institute of Technology, in 2006, 2008, and 2013, respectively. He was a Visiting Scholar with the School of Materials Science and Engineering, Georgia Institute of Technology, under the supervision of Prof. Zhong Lin Wang, from 2017 to 2018. He is currently a Professor with the School of Mechatronic Engineering, Changchun University of Technology. His research interests include triboelectric nanogenerators, piezoelectric energy harvesters, and piezoelectric actuators.

CHUANXUE SONG received the B.S., M.S., and Ph.D. degrees from the Jilin University of Technology, in 1982, 1985, and 1991, respectively. He is currently a Professor with the College of Automotive Engineering, Jilin University. His research interests include hybrid vehicle theory and control technology.